

Review

Formation of ZnO/CuO Heterostructures Based on Quasi-One-Dimensional Nanomaterials

Serguei P. Murzin ^{1,2} ¹ TU Wien, Karlsplatz 13, 1040 Vienna, Austria; serguei.murzin@tuwien.ac.at² Samara National Research University, Moskovskoe Shosse 34, 443086 Samara, Russia; murzin@ssau.ru

Abstract: Nanostructured metal oxides are of great interest both for advanced research and for a wide range of applications that contribute to the increasing demands of electronics, photonics, catalysis, sensorics, and other high-tech industries and are being actively researched and developed. One-dimensional nanocrystal arrays of copper and zinc oxides have become prominent in optoelectronic devices and energy conversion systems. However, although desirable improved properties have been demonstrated, the morphology of materials containing copper and zinc oxide nanowires is extremely sensitive to synthesis conditions and difficult to control. Studies focused on the morphology control of such quasi-one-dimensional materials are not numerous, so the consideration of this issue is still relevant. The characteristics of devices based on such oxide materials can be improved by taking advantage of nanoheterojunctions. A special feature is the possibility of forming a polycrystalline heterojunction in a system of semiconductors belonging to different crystalline syngonies. Currently, much attention is devoted to developing reliable methods of obtaining such nanomaterials, including those, based on processes exploiting novel physical effects. Possibilities of synthesis by pulse-periodic laser irradiation of arrays of quasi-one-dimensional ZnO nanostructures with varying micromorphology on metallic substrates, as well as the creation of ZnO/CuO heterostructures based on ZnO nanowires, were considered. The main distinguishing feature of this approach was the use of laser-induced vibrations to intensify diffusion processes in the solid phase of metallic materials as compared to the simple effects of laser beam heating. Expanding the area of application of the advanced method of creating oxide heterostructures requires a detailed and comprehensive study of new possibilities used to form structures with improved physical properties.



Citation: Murzin, S.P. Formation of ZnO/CuO Heterostructures Based on Quasi-One-Dimensional Nanomaterials. *Appl. Sci.* **2023**, *13*, 488. <https://doi.org/10.3390/app13010488>

Academic Editor: Guijun Bi

Received: 8 December 2022

Revised: 25 December 2022

Accepted: 26 December 2022

Published: 30 December 2022



Copyright: © 2022 by the author. Licensee MDPI, Basel, Switzerland. This article is an open access article distributed under the terms and conditions of the Creative Commons Attribution (CC BY) license (<https://creativecommons.org/licenses/by/4.0/>).

Keywords: quasi-one-dimensional nanomaterials; copper and zinc oxides; synthesis; morphology; heterostructure; formation; pulse-periodic laser irradiation; laser-induced vibrations

1. Introduction

With the development of micro- and optoelectronics, sensor and microsystems technology, requirements for the functionality and energy reduction of designed devices are increasing while reducing the weight and size of components. Therefore, research on nanomaterials that contribute to the increasing demands of electronics, photonics, catalysis, sensorics, and other high-tech industries is becoming topical [1–3]. Nanostructured metal oxides (e.g., in the form of nanowires, nanorods, nanotubes), which are being actively researched and developed, are of great interest both for promising research and for a wide range of applications. Such oxide nanomaterials demonstrate unique properties, which may be significantly superior to those of their macroscale analogs [4,5].

One of the fields for the application of metal oxides is heterogeneous catalysis, in which they are used as carriers as well as active phases [6]. Currently, in the chemical industry, there is an evident tendency for a transition from homogeneous to heterogeneous catalytic processes, so the proportion of homogeneous catalytic processes is decreasing and constitutes only about 10% [7]. In heterogeneous catalysis, unlike homogeneous catalysis, the active centres are not each molecule of the catalyst, but only the available atoms on

the surface. The requirement for a high concentration of catalytic centres in the adsorption process [8] motivates the use of nanostructured materials. The use of nanostructured metal oxides provides an opportunity to develop effective catalysts with high selectivity, stability and responsiveness [9]. Much attention has been paid to the application of synthesized one-dimensional (1D) metal oxide nanostructures. This is also facilitated by the ability to adapt the properties of metal oxides by controlling their shape, size and composition [10]. The use of metal oxide nanomaterials can also increase the selectivity of heterogeneous catalytic processes, i.e., the ability to selectively accelerate the target reaction without increasing the temperature and pressure. Due to their high surface area-to-volume ratio and inherent surface defects, these materials show the highest catalytic efficiency [11]. An example is the nanowire complex metal/metal oxide catalysts described in [12], which showed high catalytic activity in the CO oxidation reaction.

Metal oxide-based semiconductor nanowires with unique electrical, mechanical and optical properties and a high surface-to-volume ratio have become a promising and attractive base for sensor devices [13–15]. This is facilitated by the fact that in addition to good thermal and chemical stability, such materials have excellent sensitivity to changes in environmental conditions. Their gas-sensitive properties have been widely studied to detect and measure the concentration of various substances [16,17]. A smaller sensor size results in lower power consumption due to reduced thermal mass, faster heating and easier integration with small microchips. The larger effective area, which enhances gas adsorption phenomena, is a major advantage of nanostructured materials [18]. Resistive-type gas sensors are widely used to detect various toxic gases and volatile organic compounds [19–21]. Nanowires and metal oxide heterostructures are key components of future sensor devices due to their special properties [22–24]. New applications of sensors based on metal oxide semiconductor nanowires in disease diagnosis, environmental engineering, safety and security are being explored [25].

There are two main approaches for obtaining arrays of nanostructures on metal substrates. The first one involves the application and improvement of technologies developed in the semiconductor industry. Deposition and local removal of material on planar substrates is performed to reduce the size of structures to the nanometer scale. Such methods as nanoimprint [26,27], electron beam [28,29], ion beam [29,30], and scanning probe lithography [31] are utilized for the selective removal of materials. However, such nanolithography methods are mainly applied to create monolayer semiconductors and metal/metal oxide 2D patterns. In addition, their disadvantages are a relatively high cost and low productivity. The second approach makes use of the enlargement of the initial nuclei to one-dimensional nanostructures under the action of physicochemical forces. This occurs, for example, when using methods of gas-phase chemical synthesis, electrochemical deposition, crystallization from vapour or liquid phase, as well as template synthesis [32,33]. The main obstacle to the wide practical application of this approach is that the synthesis of quasi-one-dimensional nanostructures involves the creation of specific growing conditions. In addition, there is a need for further removal of the substrate (template), usually by chemical etching, which can also have a negative impact on the quality of the obtained nanostructures. Therefore, currently, the focus is on developing reliable methods of obtaining such nanomaterials, including those, based on processes exploiting novel physical effects.

A high-potential application of oxide materials is heterostructured solar power. Heterojunction solar cells or heterojunctions with intrinsic thin-layer solar cells are one fine example of such structures with high efficiency [34]. The characteristics of photodetector heterostructures can be improved by taking advantage of nanoheterojunctions. The defect-free junction of crystal lattices of the coupled materials is only possible when their type, orientation and period are the same. A special feature is the possibility of forming a polycrystalline heterojunction in a system of semiconductors belonging to different crystalline syngonies. For its implementation, it is sufficient that at least one of the faces of each lattice has close geometric parameters [35]. In [36] it has been shown that an important task at present is the development of technological methods ensuring the creation of n-ZnO/p-

CuO heterostructures formed on the basis of zinc oxide nanoobjects with arranged facets (10-10). The requirement of high surface area can be achieved by producing nanostructured layers in the form of both nanorods and nanowires.

In [37] the possibilities of synthesis by pulse-periodic laser irradiation of arrays of quasi-one-dimensional ZnO nanostructures with varying micromorphology on metallic substrates were considered. The main distinguishing feature of this approach was the use of laser-induced vibrations to intensify diffusion processes in the solid phase of metallic materials as compared to the simple effects of laser beam heating. This identified physical effect has been explained by the synergy between thermal effects and vibrations in the range of sound and infrasound frequencies, leading to a non-stationary stress-strain state. By performing laser exposure on the pre-etching surface of Cu-Zn alloy, ZnO/CuO heterostructures based on ZnO nanowires were synthesized in [38]. The synthesized structures had a high surface area-to-volume ratio and good electrical contact between the oxide layer and the electrically conducting substrate. To effectively control the thermochemical processes, systems of laser beam shaping with free-form diffractive optics, which provide a predetermined spatial redistribution of energy, have been used [39].

Expanding the area of application of the advanced method of creating oxide heterostructures requires a detailed and comprehensive study of new possibilities used to form structures with improved physical properties. The principal objective of this article is to provide systematized information on the methods of fabrication and applications of CuO- and ZnO-based nanostructures, as well as features of the formation of ZnO/CuO heterostructures based on quasi-one-dimensional nanomaterials.

2. CuO Nanowires: Fabrication Methods, Areas of Application

Copper oxide nanowires have become important in optoelectronic devices and systems for energy conversion. The methods of CuO nanowires growing include wet-chemical [40, 41], solution-based, electrochemical [42] and hydrothermal methods. The methods of thermal and plasma oxidation are also used, which are considered to be the most prospective ones from the point of view of advanced synthesis of nanowires. A combined hybrid wet chemical method in which nanowires of copper hydroxide are transformed into copper oxide by plasma oxidation is promising. According to [43] it was shown that although the desired improved properties have been demonstrated, materials containing copper oxide nanowires cannot yet be produced in large quantities, for wider use. Therefore, the search must continue for the most efficient synthesis processes that provide not only high quality and improved properties of such materials but also higher productivity. One promising approach for the growth of nanomaterials is thermal oxidation. The creation of copper oxide II (CuO) nanowires by thermal oxidation of copper in the air appears to be a simple and relatively cost-effective strategy [44,45], including the use of additional electrical or magnetic actions [46,47].

Possibilities for the practical application of copper (II) oxide nanowires continue to extend actively. For example, ref. [48] reports that a highly sensitive electrochemical sensor with CuO nanowire electrodes was fabricated on the copper substrate and used for the non-enzymatic determination of glucose. The development of high-performance gas sensors based on CuO nanowire networks demonstrating fast response/recovery times with ultra-high response is of great importance for gas sensing applications. The sensors fabricated in [49] demonstrated improved properties in the detection of ethanol vapour. Sensors based on CuO nanowires with different layer morphologies have been used for hydrogen and ammonia detection. Changing the surface morphology of the nanowires has been shown to influence the magnitude of the electrical response [50]. In [51] copper oxide II (CuO) nanowires were synthesized by thermal oxidation of copper foil (Figure 1) and deposited on fluorine-doped tin oxide-coated glass substrates. The thermal oxidation method has been shown to improve surface contact, which is promising for solar cell and catalytic applications. The use of CuO nanowires as basic components of nanoelectromechanical switches was presented in [52]. In [53], CuO nanowires demonstrated unique

characteristics with respect to the electrocatalytic oxygen extraction reaction. Arrays of CuO nanowires have been synthesized for use as the anode material in Li/Na-ion batteries [54]. Copper oxide (CuO) nanowires are an effective material for catalysis [55], including photocatalysis [56–58].

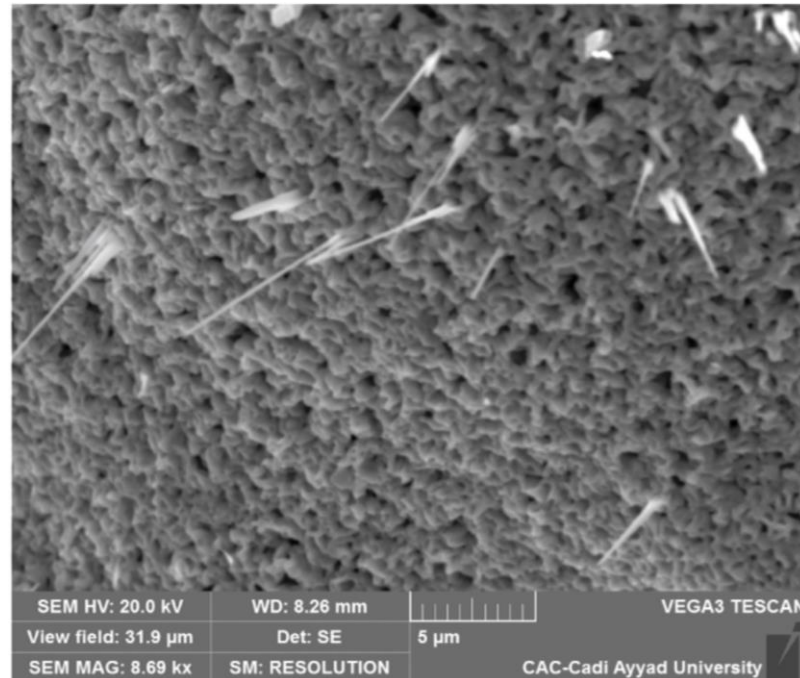


Figure 1. Scanning electron microscopy (SEM) image of CuO nanowires synthesized by thermal oxidation of copper foil at 550 °C for 4 h with a heating rate of 15 °C/min. The image shows the fragility and destruction of the nanowires at a relatively high heating rate [51].

In most cases, nanowires can be synthesized either in the supercritical liquid phase, in the vapour phase, or by thermal oxidation. The morphology of CuO nanowires, for example, can be controlled by changing the annealing temperature during thermal oxidation [59]. Nevertheless, ref. [60] shows that the growth mechanism of CuO nanowires, like other metal oxides, has yet to be fully understood. In the fabrication of CuO nanowires by thermal oxidation, even the initial thickness and configuration of the copper substrate have an influence on the morphology of the resulting CuO nanowires and electrical contact properties [61]. Geometric optimization of nanowire arrays, which is considered to be a simple and important way to improve the characteristics of photoelectrocatalytic systems based on copper oxide nanowires, has also not yet been implemented [62]. Different variants to solve this problem have been proposed. For example, in [63] laser texturing was proposed for nanowires synthesis to increase adhesion to the copper substrate before thermal oxidation. In [64] to accelerate the growth of copper oxide II (CuO) nanowires by thermal oxidation of copper surfaces, a pretreatment has been proposed to reduce the grain size of the copper substrate and increase the surface roughness. The sputtered copper surface (Figure 2), which had a fine grain structure and a significant roughness under experimental conditions demonstrated the highest nanowire density as well as the growth of quasi-one-dimensional oxide nanostructures at the lowest temperatures.

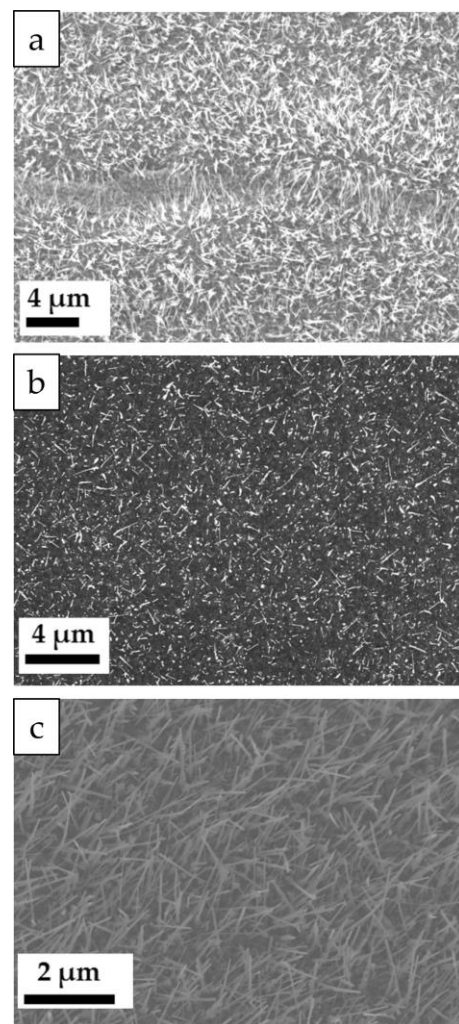


Figure 2. SEM images after heat treatment of three surfaces: copper foil (a), vapour deposited copper (b), and sputtered copper (c) [64].

3. Applications and Peculiarities of Synthesis of ZnO-Based Quasi-One-Dimensional Nanostructures

Zinc oxide is a semiconductor compound, which, due to its piezo- and segnetoelectric properties, has many practical and very promising applications [65–67]. Of particular importance is the fabrication of structures based on nanoelements such as nanowires, nanorods, nanofibres and nanofilms [68–72]. The Atomic force microscopy (AFM) images of ZnO nanofilms are shown in Figure 3 [72]. Nanostructures based on zinc oxide are used in opto- and microelectronics, as well as in microsystems technology. ZnO has potential applications in the production of light-emitting diodes and lasers in the ultraviolet spectrum, as well as in the manufacturing of solar cells, scintillators, piezoelectric devices and others [73–77].

Potential applications of ZnO nanowires in various types of solar cells have been intensively studied [78–80]. Figure 4 shows the morphological characteristics and dimensions of an ideal network of ZnO nanowires for optimal solar cell assembly [79]. Nanostructured zinc oxide has been used as a wide-band semiconductor in photoelectrochemical cells [81,82]. One-dimensional nanocrystal arrays of ZnO are a promising material for creating piezoelectric nanogenerators [83–85]. ZnO has photocatalytic efficiency and allows the degradation of contaminants in both alkaline and acidic environments [86,87]. Specific conductivity is an important factor in the photocatalysis process. Surface defects, especially oxygen defects, directly affect the photocatalytic activity of metal oxide semiconductors. Arrays of ZnO nanorods with high surface-to-volume ratios were shown in [88–90] to be

promising photocatalysts for water purification both obtained by chemical bath deposition and under hydrothermal synthesis conditions. A miniature fibre thermometer based on ZnO nanorods embedded into the tip of a ZnO nanowire has been experimentally demonstrated in [91]. Such a temperature sensor offers the advantages of compactness, stability and ease of fabrication.

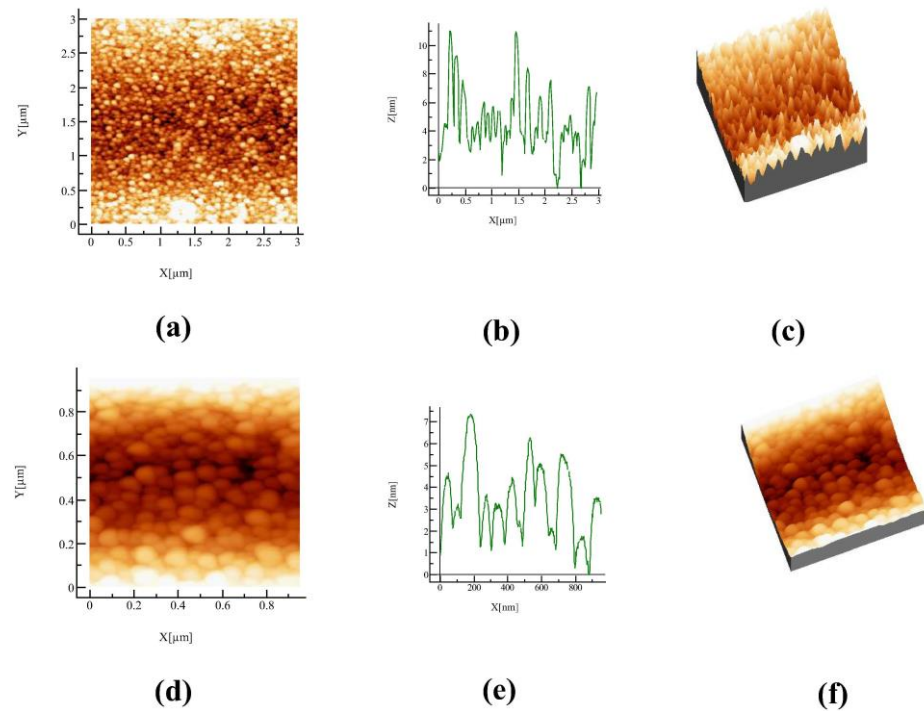


Figure 3. Atomic force microscopy (AFM) images of ZnO nanofilms (a) image $3 \times 3 \mu\text{m}^2$, (b) rough profile, (c) 3D image, (d) Zoomed image $1 \times 1 \mu\text{m}^2$, (e) rough profile, (f) 3D image [72].

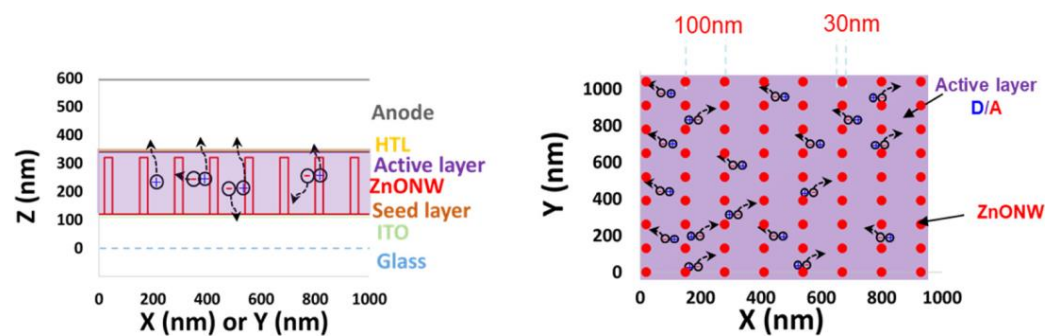


Figure 4. Morphological characteristics and dimensions of an ideal network of ZnO nanowires (ZnONW) for optimal solar cell assembly: ZnONW length ~ 200 nm, ZnONW diameter ~ 30 nm, ZnONW spacing ~ 100 nm (left) and cross-section, XY plan (right): HTL—hole transport layer; ITO—oxide layer consisting of a mixture of 90 wt% indium oxide In_2O_3 and 10 wt% tin oxide SnO_2 [79].

As a quasi-one-dimensional oxide wide-band semiconductor nanomaterial, zinc oxide nanowires, due to their high specific surface area and sufficient electrical conductivity, are used in sensor devices for the detection of hydrogen sulphide [92], hydrogen [93,94], ethanol [95–97], benzene and toluene [98]. Such devices gain distinct advantages over commercially available sensors [99–102] and provide increased selectivity and reduced energy consumption. Possible implementations of these structures include metal-oxide layered materials that can be used as materials for electrical contacts. A sensitive characteristic of ZnO nanowires in relation to the composition of the surrounding atmosphere

is electrical conductivity. The most important properties of sensors such as sensitivity, response time, and operating temperature are determined by both surface quality and structure of ZnO nanowires [103–105]. Therefore, the improvement of this area of their application, as well as others listed, directly depends on the development of methods for creating zinc oxide nanostructures with controlled predetermined properties. That is, there is a need for the controlled modification of the properties of quasi-one-dimensional zinc oxide nanostructures for specific purposes.

In [106,107], the synthesis of ZnO nanowires and nanowhiskers by direct current arc discharge between graphite cathode and graphite anode filled with ZnO in a pre-vacuumed chamber was described. Zinc oxides of diverse morphologies (nanowires, whiskers and particle agglomerates) has been synthesized on a silicon plate and a glass substrate. A modified arc process for the synthesis of a hybrid composite based not only on graphene and zinc oxide but also on copper was presented in [108]. The composite material, which combines the synergistic properties of graphene with nanostructured metals or semiconducting materials was obtained.

Arrays of ZnO nanorods/nanowires oriented vertically to the substrate have been fabricated by a direct current electrochemical method [109,110], and it has been shown that the morphology of ZnO is extremely sensitive to the synthesis conditions and is difficult to control. The morphology control of synthesised ZnO nanostructures formed on metal substrates has been discussed in [111,112]. It was shown that the performance properties of such materials tend to improve with an increase in the dispersion and uniformity of the oxide phase distribution on the metal surface. Field emission scanning electron microscopy (FE-SEM) images of ZnO nanowires grown on ITO-coated unannealed and annealed glass substrates are presented in Figure 5 [112]. In [113], ZnO nanowires were created by the hydrothermal method and the need to control their morphology was conditioned. However, studies focused on the morphology control of quasi-one-dimensional materials are not numerous, so the consideration of this issue is still relevant.

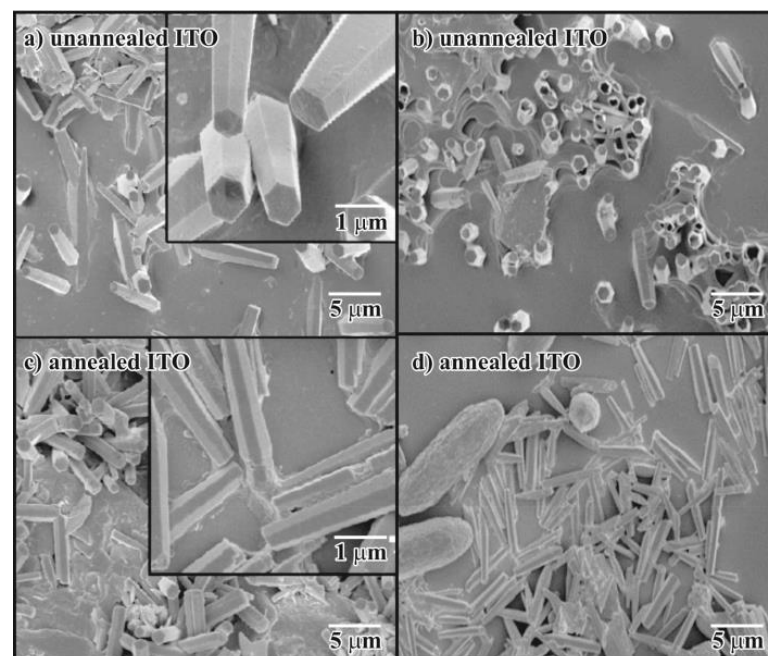


Figure 5. Field-emission scanning electron microscopy (FE-SEM) images of ZnO nanowires grown on ITO-coated glass substrates: (a,b) non annealed, (c,d) annealed. The inset images (a,c) show the side views of the ZnO nanowires [112].

4. Synthesis of ZnO/CuO Heterostructures Based on Quasi-Dimensional Nanomaterials

Unlike metals, the appearance of charge carriers in semiconductors is defined by many factors, among which the most important are the purity of the semiconductor and its

temperature [114]. Controlling the conductivity in ZnO remains an important issue. Even relatively small concentrations of intrinsic point defects and impurities can significantly affect the electrical and optical properties. As shown in [115], understanding the role of intrinsic point defects and unintentionally included shallow-donor impurities is the key to controlling the conductivity in ZnO. In optoelectronics, some progress has been made towards creating emitting p-n junctions based on ZnO nanowires by doping them. There are reports of p-type doping in ZnO [116,117]. The properties of zinc oxide-based materials can be improved by creating heterojunctions with other metal oxides. ZnO n-type nanowires combined with crystalline or polymeric p-type semiconductors are used. For instance, photocatalytic activity may be enhanced due to an increase in light absorption in the active material, a shift in absorption into the visible region of the spectrum and suppression of recombination of photoinduced charge carriers [118]. The synthesis of materials with such improved characteristics is important for the development of solar photovoltaics [119,120]. Copper oxide II (CuO), which is an indirect-gap semiconductor with p-type conductivity, can be used as a second material for heterojunction formation. As shown in [121], the formation of the ZnO/CuO p-n junction leads to an increase in photocatalytic activity due to changes in the spectral characteristics of the formed materials and more effective separation of the generated charge carriers. The self-cleaning activity of the CuO/ZnO heterostructure during photocatalysis has been demonstrated in [122]. Increased photocatalytic activity is associated with efficient separation of charge carriers due to the exploitation of the heterostructure [123].

Examples of the use of ZnO/CuO heterostructures and prospects for solar energy are presented in [124–126]. Figure 6 shows an X-ray diffraction pattern of samples from a CuO, ZnO and CuO/ZnO heterostructure synthesized by the microwave-assisted hydrothermal method [125]. In order to improve the efficiency of ZnO/CuO heterojunction photocells instead of a thin layer in [127] the use of one-dimensional ZnO structures was proposed, which provides an opportunity to increase the specific contact area of the heterojunction. In [128], a photodetector based on an array of axial n-ZnO/p-CuO heterostructure nanowires was fabricated on a Si silicon substrate by sliding angle deposition. A UV-A photodetector operating in the long-wave ultraviolet region from 320 to 400 nm showed a high rectification ratio, low dark current and fast photoresponse [129]. In [130], high-performance formaldehyde gas sensors based on ZnO/CuO heterostructure have been developed and the detection mechanism has been investigated. It has been shown that the performance of the ZnO sensor can be effectively improved by performing a heterojunction. Figure 7 shows high-resolution transmission electron microscopy images of the ZnO/CuO heterostructure [130]. ZnO/CuO heterojunction has also shown good selectivity for ethanol [131].

There is a probability that the ZnO/CuO interface is not chemically sharp. In such cases, some of the observed properties can be attributed to unintentional doping rather than heterojunction. It is assumed that CuO doping introduces an additional impurity level into the bandgap zone of ZnO. Besides, the additional CuO phase leads to a decrease in the height of the potential barriers at the surface and intergranular boundaries created due to oxygen adsorption. In these conditions, the sensitivity of the sensors to such substances as acetone vapor increases, especially under backlight conditions [132].

Controlled vapor deposition [133], the co-precipitation method [134,135], the sol-gel method [136,137], magnetron sputtering [138], thermal oxidation [139], the hydrothermal method [140], and the solvothermal method [141] have been used to produce ZnO/CuO heterojunctions. In [142], solar cell structures based on CuO/ZnO were produced by the plasma electrolyte oxidation method. The produced heterostructures are characterized by high optical absorption in the optical range due to the appropriate band gap width of CuO, which provides strong absorption in the solar spectrum region [143].

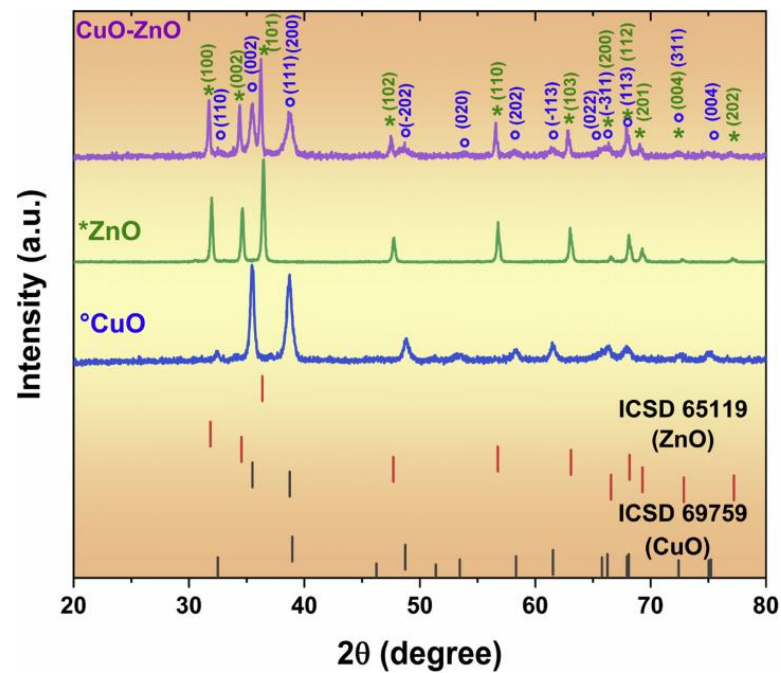


Figure 6. X-ray diffraction (XRD) pattern of samples from CuO, ZnO and CuO/ZnO heterostructure synthesized by microwave-assisted hydrothermal method [125].

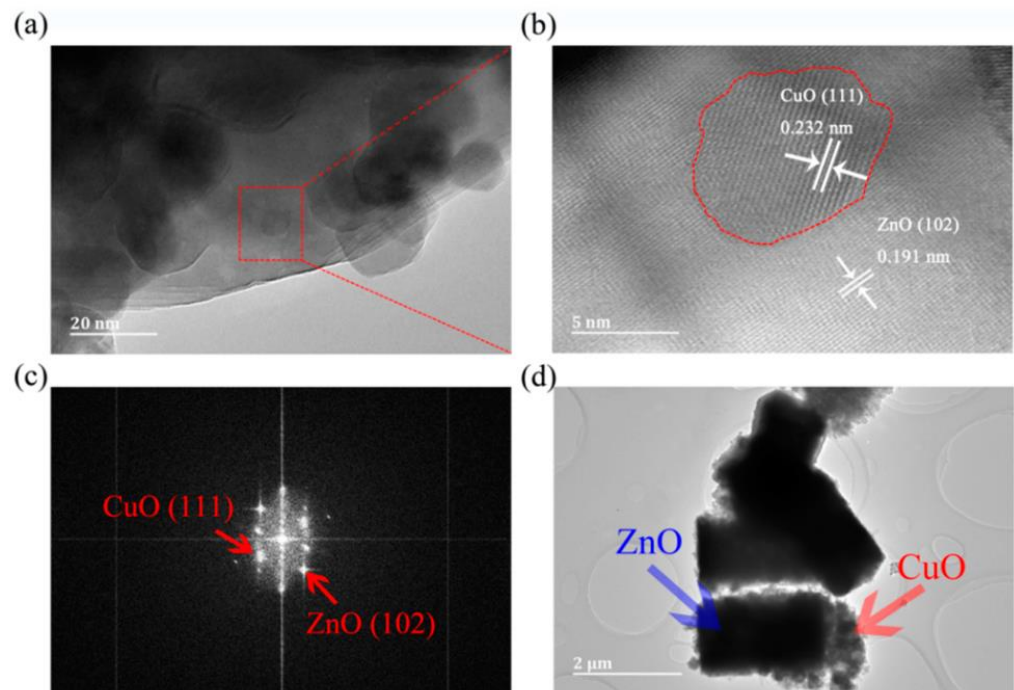


Figure 7. High-resolution transmission electron microscopy image the ZnO/CuO heterostructure: CuO particles are loaded on the surface of ZnO (a). A magnified view of the enclosed regions: The interface between ZnO and CuO particles is represented by a red dotted line (b). Fast Fourier transform (FFT) (c). Transmission electron microscopy image the ZnO/CuO heterostructure having a diameter of 1.00–1.21 μm and a height of 1.99–2.30 μm (d) [130].

The application of active layers in the form of nanowires and nanorods, which increase the transition area and improve the accumulation of charge carriers, is considered a promising way to increase the efficiency of solar cells based on CuO/ZnO heterojunctions [144]. In [145], it has been shown that bulk heterojunctions in ZnO/CuO-based solar

cells can be formed using one-dimensional ZnO nano-objects, and no ordering of arrays of such nano-objects is required. Zinc oxide has n-type conductivity, while the formation of a p-type conductivity layer is achieved by the deposition of copper oxide. CuO fills the space between the one-dimensional zinc oxide objects, creating contact with the current-carrying electrode.

The main methods for creating one-dimensional nanostructures are gas-phase deposition, in which nanocrystals grow by the vapour-liquid-crystal mechanism, liquid-phase methods, and template synthesis. Gas-phase methods of physical or chemical deposition are widely used for the synthesis of quasi-one-dimensional zinc oxide nanostructures. In this method, not only the synthesis conditions but also the specific geometry, internal tooling and other parameters of the reactor used are factors that have a strong effect on the morphology and properties of the grown ZnO nanostructures [146]. Among the liquid-phase methods of producing ZnO nanostructures are hydrothermal, using water as a solvent, solvothermal, based on the use of non-aqueous solvents, and the electrodeposition method. In general, the morphology of deposited ZnO nanostructures depends on the thickness of the seed layer and the properties of the substrate used. That is, growth mechanisms are influenced by many factors, so even small changes in synthesis conditions may lead to significant modifications in the morphology and properties of the created nanomaterials [147]. Thus, the development of reliable methods for the production of nanomaterials and heterostructures remains a topical issue.

In [148–151] new method of pulse periodic laser irradiation has been developed and a range of nanomaterials from nanoporous to layered based on ZnO nanowires have been synthesized. It was defined that a non-stationary stress-strain state caused by laser-induced vibrations is a condition for the intensification of mass transfer in the solid phase of metallic materials to be treated. A significant increase (at least 200%–300% compared to plain exposure to laser beam heating) in the diffusion coefficient in a metallic material was described [152]. The use of this identified synergistic effect of heat exposure and laser-induced vibrations made it possible to create semiconductor nanostructures on a metal substrate, including a composite material consisting of zinc oxide nanowires and copper oxide nanofilms. The formation of a crystalline structure of these semiconductors that have different conductivity types determines the creation of n-ZnO/p-CuO anisotropic heterojunction between them [38].

To create a ZnO/CuO heterostructure based on ZnO nanowires, pulsed-periodic laser irradiation on the pre-etching surface of Cu-Zn alloy has been proposed. Dezincification by etching created an alloy surface consisting of separate micrograin surfaces with high Cu content and their surrounding grain boundaries. The laser irradiation was carried out with a pulse frequency of 100 Hz; the laser power was 330 W and the diameter of the laser spot on the surface of the samples was 16 mm [38]. After such pulsed-period exposure, ZnO nanowires predominated in the grain boundary area, while the surface of each micrograin was coated with a CuO nanofilm, forming a ZnO nanowire/CuO nanofilm composite material.

Figure 8 shows a photo of the setup that has been used to study the vibration characteristics of the samples during the laser-induced formation of nanopores and nanowires [152]. Figure 9 shows a graph of the averaged over the sample surface vibration rate as a function of the sample vibration frequency during laser irradiation at a frequency of 100 Hz. Figure 10 illustrates the vibration rate distribution over the sample at a frequency equal to the laser irradiation frequency of 100 Hz. Figure 11 shows a scanning electron microscopy image of ZnO nanowires formed on the surface of Cu-Zn alloy during laser irradiation of a previously etched material [38]. It was established that the products of thermal oxidation during pulse-periodic laser irradiation are different and depend on the initial surface composition. When laser exposure was performed on a non-etching material, ZnO nanowires were formed on the porous metallic material. After surface dezincification, a composite material consisting of a network of ZnO nanowires and a CuO nanofilm on the surface of the metal material was formed by laser exposure.

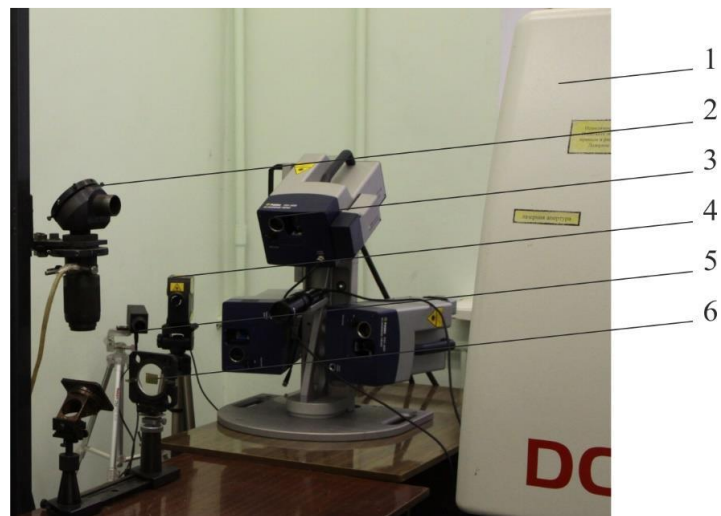


Figure 8. Photo of the setup used to study the vibration characteristics of the samples: 1—pulse-periodic laser; 2—three-coordinate scanning laser vibrometer; 3—mirror of optical system; 4—two-coordinate scanning laser vibrometer; 5—non-contact thermometer; 6—Cu-Zn alloy sample [152].

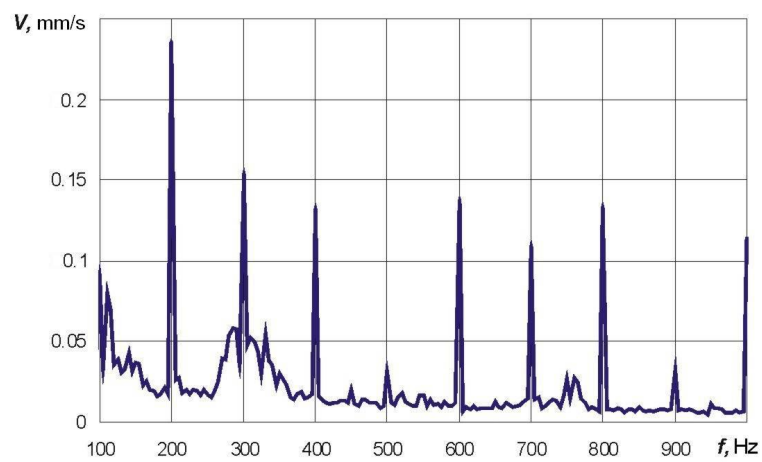


Figure 9. Graph of the averaged over the sample surface vibration rate as a function of the sample vibration frequency during laser irradiation at a frequency of 100 Hz [38].

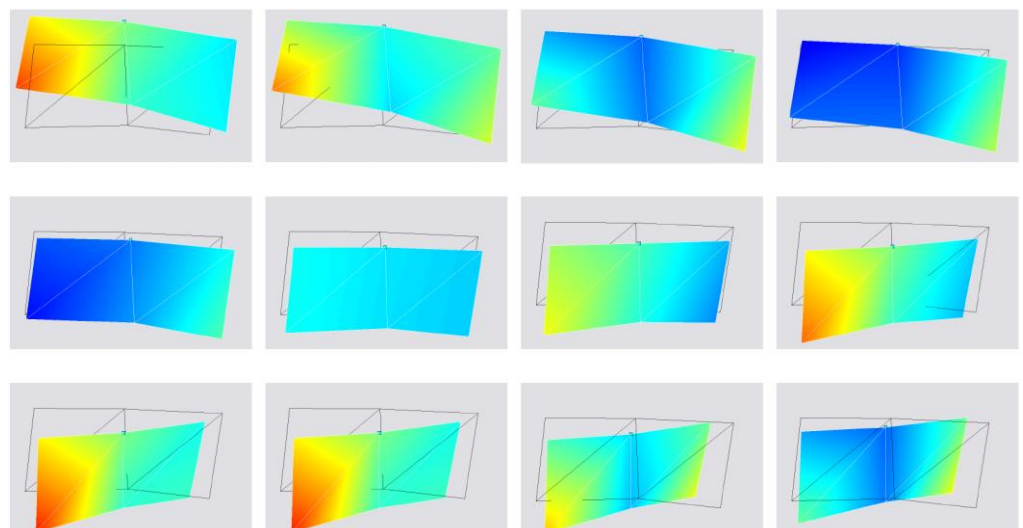


Figure 10. Cont.

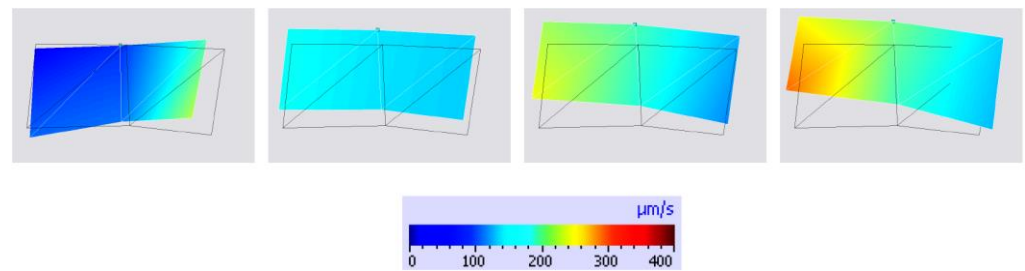


Figure 10. Re-established with PSV Presentation software, distribution of vibration rates over the sample at a frequency equal to the laser irradiation frequency of 100 Hz over the time 0.625 ms [38].

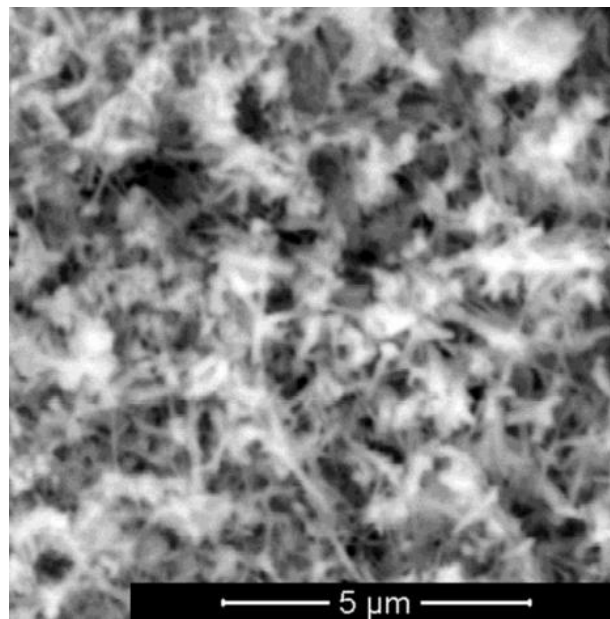


Figure 11. SEM image of ZnO nanowires formed on the surface of Cu-Zn alloy in the process of laser irradiation on the pre-etching material [38].

During experimental studies described in [153], the pulse frequency was adjusted in the range of 10–2500 Hz. The beam power was 270–330 W and the diameter of the laser spot was 20 mm. At a beam power of 270 W, the ZnO nanowires are faintly formed on the mechanically grinded surface; when the power was increased to 330 W the density of the nanowires increased considerably. However, in this case, shorter and wider nanowires are formed. The synthesized nanowires are reinforced on a substrate and have a length of $\sim 0.5\text{--}3\ \mu\text{m}$ and a diameter of $\sim 40\text{--}90\ \text{nm}$. It has been shown that ZnO predominated in the boundary area, while CuO predominated on the remaining surface. X-ray diffraction studies of copper-zinc alloy samples with an oxide semiconductor nanocomposite synthesized on the surface were carried out. Analysis of X-ray diffraction patterns showed that pulse-periodic laser irradiation leads to the formation of monoclinic CuO ($a = 4.6853\ \text{\AA}$, $b = 3.4257\ \text{\AA}$, $c = 5.1303\ \text{\AA}$, $\beta = 99.549^\circ$) and wurtzite ZnO ($a = 3.24982\ \text{\AA}$, $b = 3.24982\ \text{\AA}$, $c = 5.20661\ \text{\AA}$) on the porous Cu-Zn alloy substrate ($a = 4.256\ \text{\AA}$). Based on the specificity of oxide and zinc crystal modifications, in [154] it was shown that epitaxial relations are fulfilled for faces formed by vectors b and c . Since the mismatch of these crystal lattice parameters is relatively small, a practically defect-free heterojunction can be created [155].

5. Discussion of the Presented Results

Semiconductor heterostructures are the basis for advanced electronic and optoelectronic devices; they form the core of constructions of field-effect transistors, quantum electronics devices, computing systems, lighting technology, and electronic equipment

for communication and telecommunication systems. The combination of materials with different conductivity types is an effective approach to creating such heterostructures. The use of synergistic effects of heating and laser-induced vibrations has allowed a new approach to the formation of quasi-dimensional nanostructured metal oxides by laser-matter interaction. A new method of synthesis was developed and a number of nanomaterials ranging from nanoporous to layered metal-semiconductor based oxide-metal nanowires were synthesized by pulse-periodic laser irradiation. As a result of laser irradiation with a pulse duration in the micro- and millisecond range, the synthesis of ZnO nanowires on the surface of Cu-Zn alloy was carried out. The conditions of ZnO/CuO heterostructure formation under the laser-induced vibration were revealed and described in [38].

The possibility of synthesis of ZnO/CuO nanocomposite material by surface etching of copper-zinc substrate has been determined. Scanning electron microscopic and X-ray studies of samples after pulsed-periodic laser irradiation were performed. The method of X-ray diffraction, based on the ability of X-rays to reflect from the planes of the crystal lattice of the material, can determine in polycrystalline objects: the size of areas of coherent scattering; lattice parameters of the different fractions; the presence of chemical compounds. X-ray diffraction pattern analysis showed that oxidation during pulse-periodic laser treatment led to the formation of oxides on the surface of the becoming porous Cu-Zn alloy substrate: monoclinic CuO and wurtzite ZnO. It was found that there were differences in the structure of the surface layers of non-etching and dezincified after oxidation in the process of laser exposure. The products of oxidation in the process of pulse-periodic laser treatment depended on the initial surface composition. The laser irradiation of the non-etching material resulted in the formation of ZnO nanowires on the surface of the metallic material. On an un-zincified surface, a network of ZnO nanowires and a CuO nanofilm on the surface of the metallic material was formed by laser irradiation [153].

By varying the processing regimes and the percentage of copper and zinc components in the initial brass, for example, by reducing the zinc content, integration of 1D/1D nanomaterials such as ZnO and CuO nanowires on an electrically conductive metallic material can be implemented. Integrated 1D/1D heterostructures can be used to create a wide range of functional devices such as light-emitting diodes, rectifier transistors and diodes [156]. The difficulty is that such nanowires synthesized by pulse-periodic laser irradiation typically have random directions on the metal substrate. Their direction and spatial location are still difficult to control, and regimes for oriented structuring of highly ordered nanowires are not yet feasible.

Reliable methods for the synthesis of high-quality oxide heterostructures are still under development, the simplest fabrication method is the mechanical transfer of one 2D crystal to another using step-by-step manipulation. In [157], a method of creating 2D heterostructures is proposed where an oxide layer on a polished metal surface is deposited under controlled conditions and transferred to another substrate simply by pressing it against the target surface. Two-dimensional metal oxides that can be exfoliated are synthesized by direct oxidation of their elemental metals. The transfer technique can easily be extended to create various 2D heterostructures and devices [158]. Under elastic strain conditions [38,150–152] at which the sample is subjected, it is possible to implement regimes of mechanical exfoliation of thin layers of formed layered ZnO/CuO heterostructures from the surface of metallic material, which allows to create a 2D/2D heterostructure. It should be noted that in the area of grain boundaries, a ZnO/CuO layer is formed in which there are fractured ZnO nanowires; this layer is intensively exfoliated and chipped, revealing the unoxidized surface of Cu-Zn alloy grains [153]. As the energy or power density of the laser exposure increases, the formation time of the exfoliated layer decreases and its thickness decreases.

For new applications of electronic devices, oxide nanowires and 2D materials can also be integrated, where integration during heterostructure synthesis is the most efficient approach to combine these nanomaterials. The synthesis of an array of one-dimensional ZnO nanostructures is possible in the beginning, then the deposition of Cu nanosheet, which is subsequently oxidized to form 2D and 3D ZnO/CuO hetero-interfaces [144]. The

rectifying behaviour of the n-ZnO/p-CuO transition can be useful in photoconductive and photoactive devices, while the unipolar transport of 1D/1D thin p-CuO/n-ZnO films is useful for optical switching.

The extension of the field of application of laser irradiation as an advanced method of nanostructure formation makes it necessary to study in detail and comprehensively new possibilities of structure formation with improved physical properties. Specific features for the creation of arrays of quasi-dimensional ZnO nanostructures with different micromorphology on metal substrates are determined. Morphological characteristics are critical for many applications, so controlling these parameters by changing the synthesis conditions is an important task. This task can be solved by adaptation of the laser beam shape and redistribution of energy and power density by using appropriate optical systems. For example, the use of special optical systems based on diffractive optical elements [159,160] makes it possible to locally process the target areas with a pre-determined intensity [161,162]. The described approach opens new perspectives for the formation of oxide nanostructures to be used in heterogeneous electronics devices, optoelectronics, sensors, portable energy sources and other practical applications.

6. Conclusions

The application of nanostructured metal oxides enables increased functionality and decreased power consumption of sensor devices and microsystems, micro- and optoelectronic systems under development while reducing the mass and size of components. For this reason, such materials are of great interest, for studies as well as for a wide range of applications, and are being actively researched and developed. Much attention has been paid to the application of synthesized quasi-one-dimensional metal oxide nanostructures, including copper and zinc oxides.

The main obstacle to the wide practical application of existing physical and chemical methods for the synthesis of quasi-one-dimensional oxides is that the morphology of the deposited nanostructures depends on the thickness of the seed layer and the properties of the substrate used. Growth mechanisms are influenced by many factors, so even small changes in synthesis conditions may lead to significant modifications in the morphology and properties of the created nanomaterials. Therefore, the development of reliable methods for producing nanomaterials and heterostructures remains a topical issue.

Copper oxide nanowires have become important in optoelectronic devices and energy conversion systems. Techniques for growing copper oxide nanowires include wet-chemical, solution-based, electrochemical and hydrothermal. Thermal and plasma oxidation methods are also used. Despite the fact that the desired improved properties have been achieved, materials containing copper oxide nanowires cannot yet be produced in large quantities, for wider use. It is, therefore, necessary to continue searching for the most efficient synthesis processes that provide not only high quality and improved properties of such materials but also higher productivity.

Possible implementations of the quasi-one-dimensional structures include metal-oxide layered materials that can be used as materials for electrical contacts. The performance properties of such materials tend to improve with an increase in the dispersion and uniformity of the oxide phase distribution on the metal surface. However, the morphology of the arrays of quasi-one-dimensional materials that are synthesised on the substrate, including ZnO nanowires, is extremely sensitive to the synthesis conditions and is difficult to control, and only a few studies are devoted to this specific topic. Therefore, the consideration of this issue is still relevant.

By creating heterojunctions with other metal oxides, the properties of zinc oxide-based materials can be improved. Copper oxide (CuO), which is an indirect-gap semiconductor with p-type conductivity, can be used for heterojunction formation. Bulk heterojunctions in ZnO/CuO-based devices can be formed using one-dimensional ZnO nano-objects, and no ordering of arrays of such nano-objects is required. The formation of a p-type conductivity

layer is achieved by the deposition of copper oxide, which fills the space between the one-dimensional zinc oxide objects, creating contact with the current-carrying electrode.

The use of synergistic effects of heating and laser-induced vibrations has allowed the creation of a new approach for the formation of quasi-dimensional nanostructured metal oxides by laser-matter interaction. The condition that allows intensified mass transfer has been identified as the non-stationary stress-strain state caused by laser-induced vibrations. The knowledge of this synergetic effect—a newly identified physical effect allows significant progress in developing a novel approach for the creation of nanostructures and heterostructures of materials.

Morphological characteristics are critical for many applications, so controlling these parameters by changing the synthesis conditions is an important task. This task is solved by the adaptation of the laser beam shape and the redistribution of energy and power density by using appropriate optical systems. The presented approach opens new perspectives for the formation of oxide nanostructures to be used in heterogeneous electronics devices, optoelectronics, sensors, portable energy sources and other practical applications.

Funding: This research received no external funding.

Institutional Review Board Statement: Not applicable.

Informed Consent Statement: Not applicable.

Data Availability Statement: The data presented in this study are available in this article.

Conflicts of Interest: The author declares no conflict of interest.

References

1. Kolahalam, L.A.; Kasi Viswanath, I.V.; Diwakar, B.S.; Govindh, B.; Reddy, V.; Murthy, Y.L.N. Review on nanomaterials: Synthesis and applications. *Mater. Today Proc.* **2019**, *18*, 2182–2190. [[CrossRef](#)]
2. Zappi, D.; Ramma, M.M.; Scognamiglio, V.; Antonacci, A.; Varani, G.; Giardi, M.T. High-tech and nature-made nanocomposites and their applications in the field of sensors and biosensors for gas detection. *Biosensors* **2020**, *10*, 176. [[CrossRef](#)]
3. Diao, F.; Wang, Y. Transition metal oxide nanostructures: Premeditated fabrication and applications in electronic and photonic devices. *J. Mater. Sci.* **2018**, *53*, 4334–4359. [[CrossRef](#)]
4. Nazemi, H.; Joseph, A.; Park, J.; Emadi, A. Advanced micro- and nano-gas sensor technology: A review. *Sensors* **2019**, *19*, 1285. [[CrossRef](#)] [[PubMed](#)]
5. Malik, R.; Tomer, V.K.; Mishra, Y.K.; Lin, L. Functional gas sensing nanomaterials: A panoramic view. *Appl. Phys. Rev.* **2020**, *7*, 21301. [[CrossRef](#)]
6. Védrine, J.C. (Ed.) *Metal Oxides in Heterogeneous Catalysis*; Elsevier: Oxford, UK; Cambridge, MA, USA, 2018; 596p.
7. Rothenberg, G. *Catalysis: Concepts and Green Applications*, 2nd ed.; Wiley-VCH: Weinheim, Germany, 2017; 320p.
8. Králik, M. Adsorption, chemisorption, and catalysis. *Chem. Pap.* **2014**, *68*, 1625–1638. [[CrossRef](#)]
9. Védrine, J.C. Metal oxides in heterogeneous oxidation catalysis: State of the art and challenges for a more sustainable world. *ChemSusChem* **2019**, *12*, 577–588. [[CrossRef](#)]
10. Zhang, Q.; Wang, H.-Y.; Jia, X.; Liu, B.; Yang, Y. One-dimensional metal oxide nanostructures for heterogeneous catalysis. *Nanoscale* **2013**, *5*, 7175–7183. [[CrossRef](#)]
11. Song, H.C.; Lee, G.R.; Jeon, K.; Lee, H.; Lee, S.W.; Jung, Y.S.; Park, J.Y. Engineering nanoscale interfaces of metal/oxide nanowires to control catalytic activity. *ACS Nano* **2020**, *14*, 8335–8342. [[CrossRef](#)]
12. Xu, Y.; Cao, M.; Zhang, Q. Recent advances and perspective on heterogeneous catalysis using metals and oxide nanocrystals. *Mater. Chem. Front.* **2021**, *5*, 151–222. [[CrossRef](#)]
13. Fàbrega, C.; Casals, O.; Hernández-Ramírez, F.; Prades, J.D. A review on efficient self-heating in nanowire sensors: Prospects for very-low power devices. *Sens. Actuators B Chem.* **2018**, *256*, 797–811. [[CrossRef](#)]
14. Korotcenkov, G. Current trends in nanomaterials for metal oxide-based conductometric gas sensors: Advantages and limitations. Part 1: 1D and 2D nanostructures. *Nanomaterials* **2020**, *10*, 1392. [[CrossRef](#)] [[PubMed](#)]
15. Majhi, S.M.; Mirzaei, A.; Kim, H.W.; Kim, S.S.; Kim, T.W. Recent advances in energy-saving chemiresistive gas sensors: A review. *Nano Energy* **2021**, *79*, 105369. [[CrossRef](#)]
16. Carpenter, M.A.; Mathur, S.; Kolmakov, A. *Metal Oxide Nanomaterials for Chemical Sensors*; Springer Science & Business Media: Berlin/Heidelberg, Germany, 2012; 548p.
17. Deng, Y. *Semiconducting Metal Oxides for Gas Sensors*; Springer: Singapore, 2019; 246p.
18. Mirzaei, A.; Lee, J.-H.; Majhi, S.M.; Weber, M.; Bechelany, M.; Kim, H.W.; Kim, S.S. Resistive gas sensors based on metal-oxide nanowires. *J. Appl. Phys.* **2019**, *126*, 241102. [[CrossRef](#)]

19. Mirzaei, A.; Kim, H.W.; Kim, S.S.; Neri, G. Nanostructured semiconducting metal oxide gas sensors for acetaldehyde detection. *Chemosensors* **2019**, *7*, 56. [[CrossRef](#)]
20. Amiri, V.; Roshan, H.; Mirzaei, A.; Neri, G.; Ayeshe, A.I. Nanostructured metal oxide-based acetone gas sensors: A review. *Sensors* **2020**, *20*, 3096. [[CrossRef](#)]
21. Hung, C.M.; Le, D.T.T.; Van Hieu, N. On-chip growth of semiconductor metal oxide nanowires for gas sensors: A review. *J. Sci. Adv. Mater. Devices* **2017**, *2*, 263–285. [[CrossRef](#)]
22. Comini, E. Metal oxides nanowires chemical/gas sensors: Recent advances. *Mater. Today Adv.* **2020**, *7*, 100099. [[CrossRef](#)]
23. Nunes, D.; Pimentel, A.; Goncalves, A.; Pereira, S.; Branquinho, R.; Barquinha, P.; Fortunato, E.; Martins, R. Metal oxide nanostructures for sensor applications. *Semicond. Sci. Technol.* **2019**, *34*, 43001. [[CrossRef](#)]
24. Kim, J.-H.; Mirzaei, A.; Kim, H.W.; Kim, S.S. Variation of shell thickness in ZnO-SnO₂ core-shell nanowires for optimizing sensing behaviors to CO, C₆H₆, and C₇H₈ gases. *Sens. Actuators B Chem.* **2020**, *302*, 127150. [[CrossRef](#)]
25. Wang, Y.; Duan, L.; Deng, Z.; Liao, J. Electrically transduced gas sensors based on semiconducting metal oxide nanowires. *Sensors* **2020**, *20*, 6781. [[CrossRef](#)] [[PubMed](#)]
26. Chehadi, Z.; Bouabdellaoui, M.; Modaresialam, M.; Bottein, T.; Salvalaglio, M.; Bollani, M.; Grosso, D.; Abbarchi, M. Scalable disordered hyperuniform architectures via nanoimprint lithography of metal oxides. *ACS Appl. Mater. Interfaces* **2021**, *13*, 37761–37774. [[CrossRef](#)]
27. Jeon, S.; Sung, S.-K.; Jang, E.-H.; Jeong, J.; Surabhi, S.; Choi, J.-H.; Jeong, J.-R. Multilayer metal-oxide-metal nanopatterns via nanoimprint and strip-off for multispectral resonance. *Appl. Surf. Sci.* **2018**, *428*, 280–288. [[CrossRef](#)]
28. Wang, Y.; Kiang, K.S.; Abb, M.; Muskens, O.L.; De Groot, C.H. Electron beam lithography tri-layer lift-off to create ultracompact metal/metal oxide 2D patterns on CaF₂ substrate for surface-enhanced infrared spectroscopy. *Microelectron. Eng.* **2015**, *141*, 87–91. [[CrossRef](#)]
29. Kumar, R.; Chauhan, M.; Moinuddin, M.G.; Sharma, S.K.; Gonsalves, K.E. Development of nickel-based negative tone metal oxide cluster resists for sub-10 nm electron beam and helium ion beam lithography. *ACS Appl. Mater. Interfaces* **2020**, *12*, 19616–19624. [[CrossRef](#)]
30. Mei, H.; Koch, A.; Wan, C.; Rensberg, J.; Zhang, Z.; Salman, J.; Hafermann, M.; Schaal, M.; Xiao, Y.; Wambold, R.; et al. Tuning carrier density and phase transitions in oxide semiconductors using focused ion beams. *Nanophotonics* **2022**, *11*, 3923–3932. [[CrossRef](#)]
31. Zhao, P.; Wang, R.; Lien, D.-H.; Zhao, Y.; Kim, H.; Cho, J.; Ahn, G.H.; Javey, A. Scanning probe lithography patterning of monolayer semiconductors and application in quantifying edge recombination. *Adv. Mater.* **2019**, *31*, 1900136. [[CrossRef](#)]
32. Alameri, D.; Ocola, L.E.; Kuljanshvili, I. Controlled selective CVD growth of ZnO nanowires enabled by mask-free fabrication approach using aqueous Fe catalytic inks. *Adv. Mater. Interfaces* **2017**, *4*, 1700950. [[CrossRef](#)]
33. Qi, Z.; Li, S.; Sun, S.; Zhang, W.; Ye, W.; Fang, Y.; Tian, Y.; Dai, J.; Chen, C. Large-scale growth of density-tunable aligned ZnO nanorods arrays on GaN QDs. *Nanotechnology* **2015**, *26*, 415601. [[CrossRef](#)]
34. Sachenko, A.V.; Kryuchenko, Y.V.; Bobyl', A.V.; Kostilyov, V.P.; Terukov, E.I.; Bogdanov, D.A.; Panaiotti, I.E.; Sokolovskiy, I.O.; Orekhov, D.L. Analysis of the possibility of high-efficiency photovoltaic conversion in tandem heterojunction thin-layer solar cells. *Tech. Phys. Lett.* **2015**, *41*, 482–485. [[CrossRef](#)]
35. Lisitski, O.L.; Kumekov, M.E.; Kumekov, S.E.; Terukov, E.I. Thin-film polycrystalline n-ZnO/p-CuO heterojunction. *Semiconductors* **2009**, *43*, 765–767. [[CrossRef](#)]
36. Bobkov, A.A.; Maximov, A.I.; Moshnikov, V.A.; Somov, P.A.; Terukov, E.I. Zinc-oxide-based nanostructured materials for heterostructure solar cells. *Semiconductors* **2015**, *49*, 1357–1360. [[CrossRef](#)]
37. Murzin, S.P. Laser irradiation for enhancing mass transfer in the solid phase of metallic materials. *Metals* **2021**, *11*, 1359. [[CrossRef](#)]
38. Murzin, S.P.; Kryuchkov, A.N. Formation of ZnO/CuO heterostructure caused by laser-induced vibration action. *Procedia Eng.* **2017**, *176*, 546–551. [[CrossRef](#)]
39. Murzin, S.P.; Kazanskiy, N.L.; Stiglbrunner, C. Analysis of the advantages of laser processing of aerospace materials using diffractive optics. *Metals* **2021**, *11*, 963. [[CrossRef](#)]
40. He, C.; Cai, X.; Wei, S.-H.; Janotti, A.; Teplyakov, A.V. Self-catalyzed sensitization of CuO nanowires via a solvent-free click reaction. *Langmuir* **2020**, *36*, 14539–14545. [[CrossRef](#)]
41. Konar, S.; Kalita, H.; Puvvada, N.; Tantubay, S.; Mahto, M.K.; Biswas, S.; Pathak, A. Shape-dependent catalytic activity of CuO nanostructures. *J. Catal.* **2016**, *336*, 11–22. [[CrossRef](#)]
42. Zhang, D.; Wei, Y.; Zhao, M.; Wang, H.; Xia, Q.; Fang, Y. Facile two-step electrodeposition synthesis of CuO nanowires for ultrasensitive non-enzymatic sensing of glucose. *Int. J. Electrochem. Sci.* **2019**, *14*, 10835–10847. [[CrossRef](#)]
43. Filipič, G.; Cvelbar, U. Copper oxide nanowires: A review of growth. *Nanotechnology* **2012**, *23*, 194001. [[CrossRef](#)]
44. Wang, C.; Yang, F.; Cao, Y.; He, X.; Tang, Y.; Li, Y. Cupric oxide nanowires on three-dimensional copper foam for application in click reaction. *RSC Adv.* **2017**, *7*, 9567–9572. [[CrossRef](#)]
45. Xiang, L.; Guo, J.; Wu, C.; Cai, M.; Zhou, X.; Zhang, N. A brief review on the growth mechanism of CuO nanowires via thermal oxidation. *J. Mater. Res.* **2018**, *33*, 2264–2280. [[CrossRef](#)]
46. Shapouri, S.; Rajabi Kalvani, P.; Jahangiri, A.R.; Elahi, S.M. Physical characterization of copper oxide nanowire fabricated via magnetic-field assisted thermal oxidation. *J. Magn. Mater.* **2021**, *524*, 167633. [[CrossRef](#)]

47. Criado, D.; Zúñiga, A. Influence of an electric current on the growth kinetics of CuO nanowires produced by oxidation. *Mater. Today Commun.* **2019**, *19*, 18–22. [[CrossRef](#)]
48. Espro, C.; Donato, N.; Galvagno, S.; Aloisio, D.; Leonardi, S.G.; Neri, G. CuO nanowires-based electrodes for glucose sensors. *Chem. Eng. Trans.* **2014**, *41*, 415–420.
49. Lupan, O.; Postica, V.; Cretu, V.; Wolff, N.; Duppel, V.; Kienle, L.; Adelung, R. Single and networked CuO nanowires for highly sensitive p-type semiconductor gas sensor applications. *Phys. Status Solidi—Rapid Res. Lett.* **2016**, *10*, 260–266. [[CrossRef](#)]
50. Krawczyk, S.; Kozłowski, M.; Wronka, H.; Czerwosch, E. CuO nanowires sensor of gases. *Proc. SPIE* **2018**, *10808*, 108084K.
51. Nkhaili, L.; Narjis, A.; Agdad, A.; Tchenka, A.; El Kissani, A.; Outzourhit, A.; Oucriagli, A. A simple method to control the growth of copper oxide nanowires for solar cells and catalytic applications. *Adv. Condens. Matter Phys.* **2020**, *2020*, 5470817. [[CrossRef](#)]
52. Jasulaneca, L.; Livshits, A.I.; Meija, R.; Kosmaca, J.; Sondors, R.; Ramma, M.M.; Jevdokimovs, D.; Prikulis, J.; Erts, D. Fabrication and characterization of double- and single-clamped CuO nanowire based nanoelectromechanical switches. *Nanomaterials* **2021**, *11*, 117. [[CrossRef](#)]
53. Zuo, Y.; Liu, Y.; Li, J.; Du, R.; Han, X.; Zhang, T.; Arbiol, J.; Divins, N.J.; Llorca, J.; Guijarro, N.; et al. In situ electrochemical oxidation of Cu₂S into CuO nanowires as a durable and efficient electrocatalyst for oxygen evolution reaction. *Chem. Mater.* **2019**, *31*, 7732–7743. [[CrossRef](#)]
54. Su, Y.; Liu, T.; Zhang, P.; Zheng, P. CuO nanowire arrays synthesized at room temperature as a high-performance anode material for Li/Na-ion batteries. *Thin Solid Films* **2019**, *690*, 137522. [[CrossRef](#)]
55. Azenha, C.; Mateos-Pedrero, C.; Alvarez-Guerra, M.; Irabien, A.; Mendes, A. Enhancement of the electrochemical reduction of CO₂ to methanol and suppression of H₂ evolution over CuO nanowires. *Electrochim. Acta* **2020**, *363*, 137207. [[CrossRef](#)]
56. Kana, N.; Kaviyarasu, K.; Khamliche, T.; Magdalane, C.M.; Maaza, M. Stability and thermal conductivity of CuO nanowire for catalytic applications. *J. Environ. Chem. Eng.* **2019**, *7*, 103255. [[CrossRef](#)]
57. Yu, J.; Liao, B.; Zhang, X.; Zhou, F.; Fu, K.; Wu, X. Fabrication of CuO nanowires on copper foams by thermal oxidation and investigation of their photocatalytic properties. *Xiyou Jinshu Chin. J. Rare Met.* **2016**, *40*, 1021–1028.
58. Yan, H.; Chen, Z.; He, X.; Zhang, K.; Shen, S.; Wang, Z.; Zhou, R. Fabrication and photocatalytic performance of CuO nanowires on copper foam based on laser texturing. *Sci. Sin. Phys. Mech. Astron.* **2019**, *49*, 34209.
59. Tran, T.H.; Nguyen, M.H.; Nguyen, T.H.T.; Dao, V.P.T.; Nguyen, P.M.; Nguyen, V.T.; Pham, N.H.; Le, V.V.; Sai, C.D.; Nguyen, Q.H.; et al. Effect of annealing temperature on morphology and structure of CuO nanowires grown by thermal oxidation method. *J. Cryst. Growth* **2019**, *505*, 33–37. [[CrossRef](#)]
60. Shi, J.; Qiao, L.; Zhao, Y.; Sun, Z.; Feng, W.; Zhang, Z.; Wang, J.; Men, X. Synergistic effects on thermal growth of CuO nanowires. *J. Alloys Compd.* **2020**, *815*, 152355. [[CrossRef](#)]
61. Wang, X.; Cho, H.J. Morphologies and electrical properties of multiple CuO nanowire-based device controlled by electroplating and thermal oxidation process. *Microsyst. Technol.* **2018**, *24*, 2719–2726. [[CrossRef](#)]
62. Cao, Y.; Liu, D.; Ni, X.; Meng, X.; Zhou, Y.; Sun, Z.; Kuang, Y. Better charge separation in CuO nanowire array photocathodes: Micro-/nanostructure regulation for photoelectrochemical reaction. *ACS Appl. Energy Mater.* **2020**, *3*, 6334–6343. [[CrossRef](#)]
63. Yan, H.; Xiao, X.; Chen, Z.; Chen, Y.; Zhou, R.; Wang, Z.; Hong, M. Realization of adhesion enhancement of CuO nanowires growth on copper substrate by laser texturing. *Opt. Laser Technol.* **2019**, *119*, 105612. [[CrossRef](#)]
64. Fritz-Popovski, G.; Sosada-Ludwikowska, F.; Köck, A.; Keckes, J.; Maier, G.A. Study of CuO nanowire growth on different copper surfaces. *Sci. Rep.* **2019**, *9*, 807. [[CrossRef](#)]
65. Goel, S.; Kumar, B. A review on piezo-/ferro-electric properties of morphologically diverse ZnO nanostructures. *J. Alloys Compd.* **2020**, *816*, 152491. [[CrossRef](#)]
66. Borysiewicz, M.A. ZnO as a functional material, a review. *Crystals* **2019**, *9*, 505. [[CrossRef](#)]
67. Theerthagiri, J.; Salla, S.; Senthil, R.A.; Nithyadharseni, P.; Madankumar, A.; Arunachalam, P.; Maiyalagan, T.; Kim, H.-S. A review on ZnO nanostructured materials: Energy, environmental and biological applications. *Nanotechnology* **2019**, *30*, 392001. [[CrossRef](#)]
68. Hadis, M.; Ümit, Ö. *Zinc Oxide: Fundamentals, Materials and Device Technology*; Wiley-VCH Verlag GmbH & Co.: Weinheim, Germany, 2009; 477p.
69. Aisida, S.O.; Obodo, R.M.; Arshad, M.; Mahmood, I.; Ahmad, I.; Ezema, F.I.; Zhao, T.-K.; Malik, M. Irradiation-induced structural changes in ZnO nanowires. *Nucl. Instrum. Methods Phys. Res. B* **2019**, *458*, 61–71. [[CrossRef](#)]
70. Al-Ruqeishi, M.S.; Mohiuddin, T.; Al-Habsi, B.; Al-Ruqeishi, F.; Al-Fahdi, A.; Al-Khusaibi, A. Piezoelectric nanogenerator based on ZnO nanorods. *Arab. J. Chem.* **2019**, *12*, 5173–5179. [[CrossRef](#)]
71. Di Mauro, A.; Zimbone, M.; Fragala, M.E.; Impellizzeri, G. Synthesis of ZnO nanofibers by the electrospinning process. *Mater. Sci. Semicond.* **2016**, *42*, 98–101. [[CrossRef](#)]
72. Hamzaoui, N.; Boukhaem, A.; Ghamnia, M.; Fauquet, C. Investigation of some physical properties of ZnO nanofilms synthesized by micro-droplet technique. *Results Phys.* **2017**, *7*, 1950–1958. [[CrossRef](#)]
73. Bano, N.; Hussain, I.; Sawaf, S.; Alshammari, A.; Saleemi, F. Enhancement of external quantum efficiency and quality of heterojunction white LEDs by varying the size of ZnO nanorods. *Nanotechnology* **2017**, *28*, 245203. [[CrossRef](#)]
74. Yun, S.; Guo, T.; Li, Y.; Gao, X.; Huang, A.; Kang, L. Well-ordered vertically aligned ZnO nanorods arrays for high-performance perovskite solar cells. *Mater. Res. Bull.* **2020**, *130*, 110935. [[CrossRef](#)]
75. Galdámez-Martínez, A.; Santana, G.; Güell, F.; Martínez-Alanis, P.R.; Dutt, A. Photoluminescence of ZnO nanowires: A review. *Nanomaterials* **2020**, *10*, 857. [[CrossRef](#)]

76. Angub, M.C.M.; Vergara, C.J.T.; Husay, H.A.F.; Salvador, A.A.; Empizo, M.J.F.; Kawano, K.; Minami, Y.; Shimizu, T.; Sarukura, N.; Somintac, A.S. Hydrothermal growth of vertically aligned ZnO nanorods as potential scintillator materials for radiation detectors. *J. Lumin.* **2018**, *203*, 427–435. [[CrossRef](#)]
77. Yang, D.; Qiu, Y.; Jiang, Q.; Guo, Z.; Song, W.; Xu, J.; Zong, Y.; Feng, Q.; Sun, X. Patterned growth of ZnO nanowires on flexible substrates for enhanced performance of flexible piezoelectric nanogenerators. *Appl. Phys. Lett.* **2017**, *110*, 63901. [[CrossRef](#)]
78. Consonni, V.; Briscoe, J.; Kärber, E.; Li, X.; Cossuet, T. ZnO nanowires for solar cells: A comprehensive review. *Nanotechnology* **2019**, *30*, 362001. [[CrossRef](#)]
79. Nourdine, A.; Abdelli, M.; Charvin, N.; Flandin, L. Custom synthesis of ZnO nanowires for efficient ambient air-processed solar cells. *ACS Omega* **2021**, *6*, 32365–32378. [[CrossRef](#)]
80. Wei, Y.; Nakamura, M.; Ding, C.; Liu, D.; Li, H.; Li, Y.; Yang, Y.; Wang, D.; Wang, R.; Hayase, S.; et al. Unraveling the organic and inorganic passivation mechanism of ZnO nanowires for construction of efficient bulk heterojunction quantum dot solar cells. *ACS Appl. Mater. Interfaces* **2022**, *14*, 36268–36276. [[CrossRef](#)]
81. Saleem, M.; Farooq, W.A.; Khan, M.I.; Akhtar, M.N.; Rehman, S.U.; Ahmad, N.; Khalid, M.; Atif, M.; AlMutairi, M.A.; Irfan, M. Effect of ZnO nanoparticles coating layers on top of ZnO nanowires for morphological, optical, and photovoltaic properties of dye-sensitized solar cells. *Micromachines* **2019**, *10*, 819. [[CrossRef](#)]
82. Nicaise, S.M.; Cheng, J.J.; Kiani, A.; Gradečak, S.; Berggren, K.K. Control of zinc oxide nanowire array properties with electron-beam lithography templating for photovoltaic applications. *Nanotechnology* **2015**, *26*, 75303. [[CrossRef](#)]
83. Serairi, L.; Leprince-Wang, Y. ZnO nanowire-based piezoelectric nanogenerator device performance tests. *Crystals* **2022**, *12*, 1023. [[CrossRef](#)]
84. Sun, L.; Sun, N.; Liu, Y.; Jiang, C. A High-sensitivity knock sensor based on zno nanowires array as piezoelectric nanogenerator. *Chem. Lett.* **2021**, *50*, 1118–1122. [[CrossRef](#)]
85. Ahmad, M.; Ahmad, M.K.; Mamat, M.H.; Mohamed, A.; Suriani, A.B.; Ismail, N.M.A.N.; Soon, C.F.; Nafarizal, N. Effects of group-I elements on output voltage generation of ZnO nanowires based nanogenerator; degradation of screening effects by oxidation of nanowires. *Micromachines* **2022**, *13*, 1450. [[CrossRef](#)]
86. Mohd Adnan, M.A.; Julkapli, N.M.; Abd Hamid, S.B. Review on ZnO hybrid photocatalyst: Impact on photocatalytic activities of water pollutant degradation. *Rev. Inorg. Chem.* **2016**, *36*, 77–104. [[CrossRef](#)]
87. Zhang, Y.; Huang, X.; Yeom, J. A floatable piezo-photocatalytic platform based on semi-embedded ZnO nanowire array for high-performance water decontamination. *Nano-Micro Lett.* **2019**, *11*, 11. [[CrossRef](#)]
88. Gaffuri, P.; Dedova, T.; Appert, E.; Danilson, M.; Baillard, A.; Chaix-Pluchery, O.; Güell, F.; Oja-Acik, I.; Consonni, V. Enhanced photocatalytic activity of chemically deposited ZnO nanowires using doping and annealing strategies for water remediation. *Appl. Surf. Sci.* **2022**, *582*, 152323. [[CrossRef](#)]
89. Leprince-Wang, Y.; Martin, N.; Habba, Y.G.; Le Pivert, M.; Capochichi-Gnambodoe, M. ZnO nanostructure based photocatalysis for water purification. *NanoWorld J.* **2020**, *6*, 1–6. [[CrossRef](#)]
90. Lam, S.-M.; Sin, J.-C. A green and facile hydrothermal synthesis of ZnO nanorods for photocatalytic application. *JOJ Mater. Sci.* **2018**, *4*, 555629.
91. Cao, H.; Li, D.; Zhou, K.; Chen, Y. Demonstration of a ZnO-nanowire-based nanograting temperature sensor. *Photonic Sens.* **2023**, *13*, 230123. [[CrossRef](#)]
92. Zhu, L.-Y.; Yuan, K.-P.; Yang, J.-H.; Hang, C.-Z.; Ma, H.-P.; Ji, X.-M.; Devi, A.; Lu, H.-L.; Zhang, D.W. Hierarchical highly ordered SnO₂ nanobowl branched ZnO nanowires for ultrasensitive and selective hydrogen sulfide gas sensing. *Microsyst. Nanoeng.* **2020**, *6*, 30. [[CrossRef](#)]
93. Chowdhury, P.; Roy, S.; Banerjee, N.; Dutta, K.; Gangopadhaya, U.; Biswas, U. Facile synthesis of ZnO nanofoam on ZnO nanowire for hydrogen gas detection. *Nanosci. Nanotechnol.—Asia* **2020**, *10*, 86–92. [[CrossRef](#)]
94. Jabeen, M.; Ashraf, M.W.; Tayyaba, S.; Manzoor, S.; Javed, M.T.; Kumar, R.V.; Ahmed, M. Hydrogen gas sensing OF ZnO nanowires synthesis by hydrothermal technique. *Dig. J. Nanomater. Biostructures* **2018**, *13*, 263–269.
95. Navarrete, E.; Güell, F.; Martínez-Alanis, P.R.; Llobet, E. Chemical vapour deposited ZnO nanowires for detecting ethanol and NO₂. *J. Alloys Compd.* **2022**, *890*, 161923. [[CrossRef](#)]
96. Bertuna, A.; Faglia, G.; Ferroni, M.; Kaur, N.; Arachchige, H.M.M.M.; Sberveglieri, G.; Comini, E. Metal oxide nanowire preparation and their integration into chemical sensing devices at the SENSOR lab in Brescia. *Sensors* **2017**, *17*, 1000. [[CrossRef](#)]
97. Quy, C.T.; Hung, C.M.; Van Duy, N.; Hoa, N.D.; Jiao, M.; Nguyen, H. Ethanol-sensing characteristics of nanostructured ZnO: Nanorods, nanowires, and porous nanoparticles. *J. Electron. Mater.* **2017**, *46*, 3406–3411. [[CrossRef](#)]
98. Kim, J.-H.; Lee, J.-H.; Park, Y.; Kim, J.-Y.; Mirzaei, A.; Kim, H.W.; Kim, S.S. Toluene- and benzene-selective gas sensors based on Pt- and Pd-functionalized ZnO nanowires in self-heating mode. *Sens. Actuators B Chem.* **2019**, *294*, 78–88. [[CrossRef](#)]
99. Bhati, V.S.; Hojamberdiev, M.; Kumar, M. Enhanced sensing performance of ZnO nanostructures-based gas sensors: A review. *Energy Rep.* **2020**, *6*, 46–62. [[CrossRef](#)]
100. Campos, A.C.; Paes, S.C.; Correa, B.S.; Cabrera-Pasca, G.A.; Costa, M.S.; Costa, C.S.; Otubo, L.; Carbonari, A.W. Growth of long ZnO nanowires with high density on the ZnO surface for gas sensors. *ACS Appl. Nano Mater.* **2020**, *3*, 175–185. [[CrossRef](#)]
101. Bai, Z.; Xu, W.; Xie, C.; Dong, M.; Zhang, S.; Xu, J.; Xiao, S. Preparation and gas-sensing property of parallel-aligned ZnO nanofibrous films. *Bull. Mater. Sci.* **2013**, *36*, 505–511. [[CrossRef](#)]

102. Kang, Y.; Yu, F.; Zhang, L.; Wang, W.; Chen, L.; Li, Y. Review of ZnO-based nanomaterials in gas sensors. *Solid State Ion.* **2021**, *360*, 115544. [[CrossRef](#)]
103. Drmosh, Q.A.; Olanrewaju Alade, I.; Qamar, M.; Akbar, S. Zinc oxide-based acetone gas sensors for breath analysis: A review. *Chem. Asian J.* **2021**, *16*, 1519–1538. [[CrossRef](#)]
104. Yuan, Z.; Yin, L.; Ding, H.; Huang, W.; Shuai, C.; Deng, J. One-step synthesis of single-crystalline ZnO nanowires for the application of gas sensor. *J. Mater. Sci. Mater. Electron.* **2018**, *29*, 11559–11565. [[CrossRef](#)]
105. Tamvakos, A.; Calestani, D.; Tamvakos, D.; Pullini, D.; Sgroi, M.; Pruna, A. Low concentration CO gas sensing properties of hybrid ZnO architecture. *Microelectron. Eng.* **2016**, *160*, 12–17. [[CrossRef](#)]
106. Konstantinova, M.; Koprinarov, N.; Tzacheva, T.Z. Arc discharge assisted synthesis of ZnO whiskers and nanowires. *Optoelectron. Adv. Mater. Rapid Commun.* **2010**, *4*, 1709–1712.
107. Koprinarov, N.; Marinov, M.; Konstantinova, M. An arc discharge by closely situated electrodes for synthesis of nanostructures. *Solid State Phenom.* **2010**, *159*, 181–184. [[CrossRef](#)]
108. Kane, A.; Hinkov, I.; Brinza, O.; Hosni, M.; Barry, A.H.; Cherif, S.M.; Farhat, S. One-step synthesis of graphene, copper and zinc oxide graphene hybrids via arc discharge: Experiments and modeling. *Coatings* **2020**, *10*, 308. [[CrossRef](#)]
109. Ahmad, R.; Majhi, S.M.; Zhang, X.; Swager, T.M.; Salama, K.N. Recent progress and perspectives of gas sensors based on vertically oriented ZnO nanomaterials. *Adv. Colloid Interface Sci.* **2019**, *270*, 1–27. [[CrossRef](#)]
110. Huang, Y.M.; Ma, Q.-L.; Zhai, B.-G. Controlled morphology of ZnO nanostructures by adjusting the zinc foil heating temperature in an air-filled box furnace. *Mater. Chem. Phys.* **2014**, *147*, 788–795. [[CrossRef](#)]
111. Cossuet, T.; Roussel, H.; Chauveau, J.-M.; Chaix-Pluchery, O.; Thomassin, J.-L.; Appert, E.; Consonni, V. Well-ordered ZnO nanowires with controllable inclination on semipolar ZnO surfaces by chemical bath deposition. *Nanotechnology* **2018**, *29*, 475601. [[CrossRef](#)]
112. Paiman, S.; Hui Ling, T.; Husham, M.; Sagadevan, S. Significant effect on annealing temperature and enhancement on structural, optical and electrical properties of zinc oxide nanowires. *Results Phys.* **2020**, *17*, 103185. [[CrossRef](#)]
113. Mateen Tantray, A.; Shah, M.A. Photo electrochemical ability of dense and aligned ZnO nanowire arrays fabricated through electrochemical anodization. *Chem. Phys. Lett.* **2020**, *747*, 137346. [[CrossRef](#)]
114. Kasap, S.; Koughia, C.; Ruda, H.; Johanson, R. Electrical Conduction in Metals and Semiconductors. In *Springer Handbook of Electronic and Photonic Materials*; Kasap, S., Capper, P., Eds.; Springer: Boston, MA, USA, 2006; pp. 19–45.
115. Janotti, A.; Van De Walle, C.G. Fundamentals of zinc oxide as a semiconductor. *Rep. Prog. Phys.* **2009**, *72*, 126501. [[CrossRef](#)]
116. Saha, R.; Saha, N.R.; Karmakar, A.; Dalapati, G.K.; Chattopadhyay, S. Generation of oxygen interstitials with excess in situ Ga doping in chemical bath deposition process for the growth of p-type ZnO nanowires. *J. Mater. Sci. Mater. Electron.* **2019**, *30*, 8796–8804. [[CrossRef](#)]
117. Tsay, C.-Y.; Hsiao, I.-P.; Chang, F.-Y.; Hsu, C.-L. Improving the photoelectrical characteristics of self-powered p-GaN film/n-ZnO nanowires heterojunction ultraviolet photodetectors through gallium and indium co-doping. *Mater. Sci. Semicond.* **2021**, *121*, 105295. [[CrossRef](#)]
118. Kumari, V.; Yadav, S.; Jindal, J.; Sharma, S.; Kumari, K.; Kumar, N. Synthesis and characterization of heterogeneous ZnO/CuO hierarchical nanostructures for photocatalytic degradation of organic pollutant. *Adv. Powder Technol.* **2020**, *31*, 2658–2668. [[CrossRef](#)]
119. Tan, H.; Huang, Z.; Wang, Y.; Sang, L.; Wang, L.; Jia, F.; Sun, F.; Wang, X. One-step fabrication and photocatalytic performance of sea urchin-like CuO/ZnO heterostructures. *New J. Chem.* **2022**, *46*, 16078–16089. [[CrossRef](#)]
120. Lashkova, N.A.; Maximov, A.I.; Ryabko, A.A.; Bobkov, A.A.; Moshnikov, V.A.; Terukov, E.I. Synthesis of ZnO-based nanostructures for heterostructure photovoltaic cells. *Semiconductors* **2016**, *50*, 1254–1260. [[CrossRef](#)]
121. Li, Z.; Jia, M.; Abraham, B.; Blake, J.C.; Bodine, D.; Newberg, J.T.; Gundlach, L. Synthesis and characterization of ZnO/CuO vertically aligned hierarchical tree-like nanostructure. *Langmuir* **2018**, *34*, 961–969. [[CrossRef](#)]
122. Upadhaya, D.; Dhar Purkayastha, D. Self-cleaning activity of CuO/ZnO heterostructure: A synergy of photocatalysis and hydrophilicity. *J. Taiwan Inst. Chem. Eng.* **2022**, *132*, 104216. [[CrossRef](#)]
123. Meng, Q.; Liu, W.; Jiang, J.; Zhang, X. Fabrication of novel p-CuO/n-ZnO heterojunction nanofibers by electrospinning for enhanced photocatalytic performance in the denitrification of fuel oil. *Ceram. Int.* **2021**, *47*, 19402–19413. [[CrossRef](#)]
124. Karimi Shamsabadi, M.; Behpour, M. Fabricated CuO–ZnO/nanozeolite X heterostructure with enhanced photocatalytic performance: Mechanism investigation and degradation pathway. *Mater. Sci. Eng. B Solid-State Mater. Adv. Technol.* **2021**, *269*, 115170. [[CrossRef](#)]
125. Oliveira, M.C.; Fonseca, V.S.; Andrade Neto, N.F.; Ribeiro, R.A.P.; Longo, E.; de Lazaro, S.R.; Motta, F.V.; Bomio, M.R.D. Connecting theory with experiment to understand the photocatalytic activity of CuO–ZnO heterostructure. *Ceram. Int.* **2020**, *46*, 9446–9454. [[CrossRef](#)]
126. Bajiri, M.A.; Hezam, A.; Namratha, K.; Viswanath, R.; Drmosh, Q.A.; Bhojya Naik, H.S.; Byrappa, K. CuO/ZnO/g-C₃N₄ heterostructures as efficient visible light-driven photocatalysts. *J. Environ. Chem. Eng.* **2019**, *7*, 103412. [[CrossRef](#)]
127. Peshkova, T.V.; Dimitrov, D.T.; Nalimova, S.S.; Kononova, I.E.; Nikolaev, N.K.; Papazova, K.I.; Bozhinova, A.S.; Moshnikov, V.A.; Terukov, E.I. Structures of nanowires with Zn-ZnO:CuO junctions for detecting ethanol vapors. *Tech. Phys.* **2014**, *59*, 771–776. [[CrossRef](#)]

128. Daimary, S.; Dhar, J.C. Ultrafast photoresponse using axial n-ZnO/p-CuO heterostructure nanowires array-based photodetectors. *IEEE Trans. Electron Devices* **2022**, *69*, 3768–3774. [[CrossRef](#)]
129. Daimary, S.; Chetri, P.; Dhar, J.C. High performance UV-A detector using axial n-ZnO/p-CuO p-n junction heterostructure nanowire arrays. *IEEE Electron Device Lett.* **2022**, *43*, 898–901. [[CrossRef](#)]
130. Liu, J.; Chen, Y.; Zhang, H. Study of highly sensitive formaldehyde sensors based on ZnO/CuO heterostructure via the sol-gel method. *Sensors* **2021**, *21*, 4685. [[CrossRef](#)]
131. Cai, L.; Li, H.; Zhang, H.; Fan, W.; Wang, J.; Wang, Y.; Wang, X.; Tang, Y.; Song, Y. High performance gas sensor based on ZnO/CuO heterostructures. *Lect. Notes Electr. Eng.* **2021**, *726*, 191–198.
132. Miao, Y.; Pan, G.; Sun, C.; He, P.; Cao, G.; Luo, C.; Zhang, L.; Li, H. Enhanced photoelectric responses induced by visible light of acetone gas sensors based on CuO-ZnO nanocomposites at about room temperature. *Sens. Rev.* **2018**, *38*, 311–320. [[CrossRef](#)]
133. Khan, M.A.; Nayan, N.; Ahmad, M.K.; Fhong, S.C.; Mohamed Ali, M.S.; Mustafa, M.K.; Tahir, M. Interface study of hybrid CuO nanoparticles embedded ZnO nanowires heterojunction synthesized by controlled vapor deposition approach for optoelectronic devices. *Opt. Mater.* **2021**, *117*, 111132. [[CrossRef](#)]
134. Ren, S.; Fan, X.; Shang, Z.; Shoemaker, W.R.; Ma, L.; Wu, T.; Li, S.; Klinghoffer, N.B.; Yu, M.; Liang, X. Enhanced catalytic performance of Zr modified CuO/ZnO/Al₂O₃ catalyst for methanol and DME synthesis via CO₂ hydrogenation. *J. CO₂ Util.* **2020**, *36*, 82–95. [[CrossRef](#)]
135. Wang, G.; Mao, D.; Guo, X.; Yu, J. Enhanced performance of the CuO-ZnO-ZrO₂ catalyst for CO₂ hydrogenation to methanol by WO₃ modification. *Appl. Surf. Sci.* **2018**, *456*, 403–409. [[CrossRef](#)]
136. Tangcharoen, T.; Klysubun, W.; Kongmark, C. Synthesis and characterization of nanocrystalline CuO/ZnO composite powders with enhanced photodegradation performance under sunlight irradiation. *J. Mater. Sci. Mater. Electron.* **2020**, *31*, 12807–12822. [[CrossRef](#)]
137. Xu, L.; Su, J.; Zheng, G.; Zhang, L. Enhanced photocatalytic performance of porous ZnO thin films by CuO nanoparticles surface modification. *Mater. Sci. Eng. B Solid-State Mater. Adv. Technol.* **2019**, *248*, 114405. [[CrossRef](#)]
138. Costas, A.; Florica, C.; Preda, N.; Besleaga, C.; Kuncser, A.; Enculescu, I. Self-connected CuO–ZnO radial core–shell heterojunction nanowire arrays grown on interdigitated electrodes for visible-light photodetectors. *Sci. Rep.* **2022**, *12*, 6834. [[CrossRef](#)]
139. Arafat, M.M.; Haseeb, A.S.M.A.; Rozali, S.; Brabazon, D.; Rahman, B.M.A.; Grattan, K.T.V.; Naher, S. Synthesis of ZnO and CuO nanowires by thermal oxidation on metallic substrates. *Key Eng. Mater.* **2022**, *926*, 1703–1712. [[CrossRef](#)]
140. Cai, L.; Li, H.; Zhang, H.; Fan, W.; Wang, J.; Wang, Y.; Wang, X.; Tang, Y.; Song, Y. Enhanced performance of the tangerines-like CuO-based gas sensor using ZnO nanowire arrays. *Mater. Sci. Semicond. Process.* **2020**, *118*, 105196. [[CrossRef](#)]
141. Park, S.; Kim, S.; Kheel, H.; Hyun, S.K.; Jin, C.; Lee, C. Enhanced H₂S gas sensing performance of networked CuO-ZnO composite nanoparticle sensor. *Mater. Res. Bull.* **2016**, *82*, 130–135. [[CrossRef](#)]
142. Thu, P.T.; Thinh, V.D.; Lam, V.D.; Bach, T.N.; Phong, L.T.H.; Tung, D.H.; Manh, D.H.; Van Khien, N.; Anh, T.X.; Le, N.T.H. Decorating of Ag and CuO on ZnO nanowires by plasma electrolyte oxidation method for enhanced photocatalytic efficiency. *Catalysts* **2022**, *12*, 801. [[CrossRef](#)]
143. Guo, X.; Diao, P.; Xu, D.; Huang, S.; Yang, Y.; Jin, T.; Wu, Q.; Xiang, M.; Zhang, M. CuO/Pd composite photocathodes for photoelectrochemical hydrogen evolution reaction. *Int. J. Hydrog. Energy* **2014**, *39*, 7686–7696. [[CrossRef](#)]
144. Rahmati, A.; Zakeri-Afshar, S. Heteroepitaxial ZnO/CuO thin film and nanorods array: Photoconductivity and field emission effect. *J. Mater. Sci. Mater. Electron.* **2017**, *28*, 13032–13040. [[CrossRef](#)]
145. Bobkov, A.A.; Lashkova, N.A.; Maximov, A.I.; Moshnikov, V.A.; Nalimova, S.S. Fabrication of oxide heterostructures for promising solar cells of a new generation. *Semiconductors* **2017**, *51*, 61–65. [[CrossRef](#)]
146. Rackauskas, S. (Ed.) *Nanowires—Synthesis, Properties and Applications*; IntechOpen: London, UK, 2019; 122p.
147. Lausecker, C.; Salem, B.; Baillin, X.; Consonni, V. Implementing the reactor geometry in the modeling of chemical bath deposition of ZnO nanowires. *Nanomaterials* **2022**, *12*, 1069. [[CrossRef](#)]
148. Kazanskiy, N.L.; Murzin, S.P.; Osetrov, Y.L.; Tregub, V.I. Synthesis of nanoporous structures in metallic materials under laser action. *Opt. Lasers Eng.* **2011**, *49*, 1264–1267. [[CrossRef](#)]
149. Murzin, S.P. Exposure to laser radiation for creation of metal materials nanoporous structures. *Opt. Laser Technol.* **2013**, *48*, 509–512. [[CrossRef](#)]
150. Murzin, S.P. Formation of nanoporous structures in metallic materials by pulse-periodic laser treatment. *Opt. Laser Technol.* **2015**, *72*, 48–52. [[CrossRef](#)]
151. Murzin, S.P. Improvement of thermochemical processes of laser-matter interaction and optical systems for wavefront shaping. *Appl. Sci.* **2022**, *12*, 12133. [[CrossRef](#)]
152. Murzin, S.P.; Kazanskiy, N.L. Arrays formation of zinc oxide nano-objects with varying morphology for sensor applications. *Sensors* **2020**, *20*, 5575. [[CrossRef](#)]
153. Murzin, S.P.; Afanasiev, S.A.; Blokhin, M.V. Pulse-periodic laser action to create an ordered heterogeneous structure based on copper and zinc oxides. *J. Phys. Conf. Ser.* **2018**, *1096*, 12139. [[CrossRef](#)]
154. Adilov, S.R.; Kumekov, M.E.; Kumekov, S.E.; Terukov, E.I. Model of the formation of a polycrystalline n-ZnO/p-CuO heterojunction. *Semiconductors* **2013**, *47*, 655–656. [[CrossRef](#)]
155. Kampara, R.K.; Sonia, T.; Jeyaprakash, B.G. CuO/ZnO heterojunction nanograins: Methanol vapour detection. *J. Electron. Mater.* **2021**, *50*, 2482–2495. [[CrossRef](#)]

156. Wang, P.; Jia, C.; Huang, Y.; Duan, X. Van der Waals heterostructures by design: From 1D and 2D to 3D. *Matter* **2021**, *4*, 552–581. [[CrossRef](#)]
157. Zhang, B.Y.; Xu, K.; Yao, Q.; Jannat, A.; Ren, G.; Field, M.R.; Wen, X.; Zhou, C.; Zavabeti, A.; Ou, J.Z. Hexagonal metal oxide monolayers derived from the metal–gas interface. *Nat. Mater.* **2021**, *20*, 1073–1078. [[CrossRef](#)]
158. Parkinson, G.S. Adding oxides to the 2D toolkit. *Nat. Mater.* **2021**, *20*, 1041–1042. [[CrossRef](#)]
159. Doskolovich, L.L.; Mingazov, A.A.; Byzov, E.V.; Skidanov, R.; Ganchevskaya, S.; Bykov, D.A.; Bezus, E.A.; Podlipnov, V.V.; Porfirev, A.P.; Kazanskiy, N.L. Hybrid design of diffractive optical elements for optical beam shaping. *Opt. Express* **2021**, *29*, 31875–31890. [[CrossRef](#)]
160. Kharitonov, S.I.; Doskolovich, L.L.; Kazanskiy, N.L. Solving the inverse problem of focusing laser radiation in a plane region using geometrical optics. *Comput. Opt.* **2016**, *40*, 439–450. [[CrossRef](#)]
161. Murzin, S.P.; Kazanskiy, N.L. Use of diffractive optical elements for beam intensity redistribution. *Proc. SPIE* **2020**, *11516*, 115160H.
162. Murzin, S.P.; Kazanskiy, N.L. Study of the beam intensity redistribution in the focal plane of diffractive optical element. *Proc. SPIE* **2019**, *11146*, 111460V.

Disclaimer/Publisher’s Note: The statements, opinions and data contained in all publications are solely those of the individual author(s) and contributor(s) and not of MDPI and/or the editor(s). MDPI and/or the editor(s) disclaim responsibility for any injury to people or property resulting from any ideas, methods, instructions or products referred to in the content.